ELSEVIER

Journal of Molecular Catalysis A: Chemical 107 (1996) 175–183

JOURNAL OF MOLECULAR CATALYSIS A: CHEMICAL

Fe-pillared clays: a combination of zeolite shape selectivity and iron activity in the CO hydrogenation reaction

M. Josefina Pérez Zurita [a,*], Gerardo Vitale [a], Mireya R. de Goldwasser [a], Daysi Rojas [b], Juan J. García [b]

[a] *Centro de Catálisis, Petróleo y Petroquímica, Escuela de Química, Facultad de Ciencias, Universidad Central de Venezuela, Apartado Postal 47102, Caracas, Venezuela*

[b] *INTEVEP S.A. Apartado Postal 76343, Caracas, Venezuela*

Abstract

Fe-pillared clays (Fe-PILC) were prepared by the standard method using the complex $[Fe_3(CH_3COO)_7OH \cdot 2H_2O]^+NO_3^-$ as iron precursor. The temperature, time and iron concentration were varied during the exchange process. A thorough characterisation was carried out using XRD, textural properties, chemical analysis, scanning electron microscopy and Mössbauer spectroscopy as main techniques. The Fe-pillared clays synthesized attained remarkable thermal stability in N_2 and air (700°C), surface areas between 200 and 270 $m^2\ g^{-1}$ and basal spacing of around 21 Å when dried at room temperature. The high thermal stability reached with these solids limited the catalytic activity. However, this unwanted control of activity renders the solids selective towards the C_2–C_4 fraction of products in the CO hydrogenation reaction. Up to now, the use of Fe-pillared clays in this reaction is only found in the patent literature. The present work seeks to shed light on the behaviour of this type of solids in this reaction.

Keywords: Iron; Pillared clays; Zeolite shape selectivity; Selectivity; Carbon monoxide; Hydrogenation

1. Introduction

Pillared interlayer clays have been used as catalysts in numerous studies [1–14]. The main utility of this type of solid comes from the fact that a controlled porosity can be generated by incorporating several elements in between the layers of an expandable clay. The newly formed porous material can be systematically regulated by varying the size, the form and the distance between the exchanging cations.

Two strategies have been explored in the use of PILC in catalysis; (i) as support for the active phase; and (ii) by having the active phase forming the pillar itself.

Certain polynuclear species are of great interest because after dehydroxylation and dehydration, they can give interesting catalytic properties. An example is given by Fe-PILC where a better definition on the product distribution in the CO hydrogenation reactions is expected.

* Corresponding author.

SSDI 1381-1169(95)00218-9

Two type of precursors have been used for the synthesis of Fe-PILC: inorganic salts [11,12,15,16] and organometallic complexes [17–24]. The first Fe-PILC were reported by Berkheiser et al. [17] in 1977 and then by Traynor et al. [18] in 1978. Their main problem was the lack of thermal stability because when heated at 150°C the basal spacing decreased from 18 Å to 12 Å and their structure collapsed completely at 250°C. This lack of thermal stability was solved by Loeppert et al. [19] incorporating an excess of complex in such a way that the cation exchange capacity (CEC) were of around two, obtaining basal spacing of 17.7 Å for montmorillonite based solids and 28.5 Å for vermiculite based solids. The thermal stability of these solids was good (550°C) but the surface area was very low (20 to 60 m^2/g).

Yamanaka et al. [20] in 1984 presented the first reference related to the preparation of Fe-PILC using an aqueous solution of $[Fe_3CH_3COO)_7OH \cdot 2H_2O]^+NO_3^-$. The authors demonstrated that solids prepared from hydroxylated solutions of iron did not posses thermal stability at temperatures below 300°C. The lack of thermal stability was attributed to the fact that the Fe(III) hydroxides were not stable in water therefore, they could be removed during the washing step. To solve this problem, Yamanaka prepared an Fe-PILC exchanging a Na-montmorillonite with partially hydrolyzed trinuclear iron acetate. After calcination at 500°C, these solids presented surface areas of 280 m^2/g and basal spacing of 16.7 Å. After this paper of Yamanaka, several authors [20–24] reported the synthesis of Fe-PILC with similar characteristics of those reported by him.

The catalytic activity of Fe-PILC has been little studied. Very few works can be found in the open literature where these solids are used as catalysts [11,25] and only one patent reports it use in the CO hydrogenation reaction [26].

In the present work we report the preparation, characterisation and catalytic behaviour of Fe-PILC in the CO hydrogenation reaction.

2. Experimental

The complex $[Fe_3(CH_3COO)_7OH \cdot 2H_2O]^+NO_3^-$ was synthesised using the method reported by Yamanaka et al. [20]. The iron precursor for this preparation was $Fe(NO_3)_3 9H_2O$ (Mallinckrodt). For the preparation of the PILC, a commercial montmorillonite was used (Baroid) and the standard method was conducted varying the temperature, time and iron concentration during the exchange process. After the exchange process was completed, the solids were thoroughly washed with deionized water to avoid the presence of the iron complex outside the structure. The following general formula will be used to designate the solids prepared: ${}^tP_n^T$ where t is the time of exchange, T is the temperature of exchange and n is the meq complex/g clay ratio. Thermal stability was evaluated in air atmosphere. The complex was characterised by elemental analysis using a 2400 CHN Elemental Analyser and by FTIR using a Perkin Elmer Spectrometer. The XRD analyses were conducted in a diffractometer Philips PW1730-10 fitted with a Cu tube. After washing the samples were impregnated on a glass slice. The textural properties were assessed in a Micromeritics Accelerated Surface Area and Porosimetry 2400 (ASAP 2400) apparatus and the chemical analyses were carried out in an spectrometer Varian Techtron AA-6. The transmission electron microscopy was conducted in a Hitachi H-800 equipment and the samples were prepared using a solution of ethanol and water. The suspension was placed over a copper grid and covered with carbon. Mössbauer spectroscopy was carried out in zero field at room temperature. The gamma source was ^{57}Co immersed in a Pd matrix. The isomer shifts are quoted relative to an α-Fe absorber. The catalytic test were conducted under mild conditions, 300°C and 300 psi. Prior to reaction, all the catalysts were calcined in steps in flowing air as follows: 100°C for 6 h, 300°C for 14 h and finally 500°C for 5 h. After calcination the

solids were reduced at 450°C under flowing hydrogen for 16 h.

3. Results

3.1. Characterisation of the Fe-complex

Table 1 shows the elemental analysis carried out for the characterisation of the iron complex. It can be observed that the results obtained are within the expected values. Similar results were reported by Yamanaka et al. [20]. Additionally, an FTIR spectrum of the Fe-complex was taken to further characterise the complex. Fig. 1 shows the infrared spectrum obtained. The complex spectrum shows a signal at 1687.8 cm^{-1} assigned to the N=O double bond of nitrate. The two very intense bands at 1609 and 1457.2 cm^{-1} are assigned to the symmetric and asymmetric stretching of the COO^- ion respectively and the small band situated at 1386.3 cm^{-1} is attributed to the symmetric deformation of the CH_3 groups. Signals due to the C–O bond in the acetate groups were observed at 1290.5 cm^{-1} and 1035.2 cm^{-1} [27].

3.2. Preparation of the Fe-PILC

A systematic study of the optimal conditions for pillaring the clay with the Fe-complex was conducted by varying the exchange temperature, time and meq complex/g of clay ratio.

3.3. Influence of exchange temperature

Table 2 shows the effect of temperature when preparing the Fe-PILC.

Table 1
Elemental analyses of the Fe complex

	Carbon %	Hydrogen %	Nitrogen %
Experimental [a]	23.25	4.04	1.80
Theoretical [a]	23.16	3.77	2.01
Yamanaka [20] [a]	23.49	3.93	1.97

[a] $[Fe_3(CH_3COO)_7OH \cdot 2H_2O]^+ NO_3^-$.

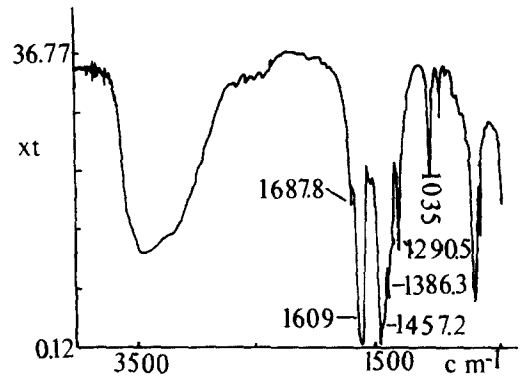

Fig. 1. I.R. spectrum of $[Fe_3(CH_3COO)_7OH \cdot 2H_2O]^+ NO_3^-$ complex.

The solid prepared using 40°C as exchange temperature showed maximum thermal stability and basal spacing. For lower temperatures, the solids are less stable thermally reaching a point when no thermal stability is observed (e.g. 20°C). When exchange temperature is higher the solid has lower thermal stability.

3.4. Influence of exchange time

The variation of basal space and thermal stability with exchange time was studied between 1 and 4 h. Table 3 shows the values obtained.

After only 1 h of exchange, the clay was already modified as seen by the increase of the basal spacing. With increasing time, no further changes were observed. The highest value after having been calcined at 500°C was obtained for the solid prepared with 3 h of exchange time.

Table 2
Basal spacing in Å and its evolution with thermal treatment of the iron-pillared clays prepared. Influence of exchange temperature

Solid	Temperature (°C)		
	25	300	500
Original clay	14.9		9.6
$^3P^{50}_{3.5}$	21.1	17.2	17.1
$^3P^{40}_{3.5}$	21.0	17.9	18.0
$^3P^{30}_{3.5}$	20.8	16.7	17.4
$^3P^{20}_{3.5}$	21.8	–	–

Table 3
Basal spacing in Å and its evolution with thermal treatment of the iron-pillared clays prepared. Influence of exchange time

Solid	Temperature (°C)		
	25	300	500
Original clay	14.9		9.6
${}^{1}P^{40}_{3.5}$	21.3	17.2	17.7
${}^{2}P^{40}_{3.5}$	20.8	17.0	17.2
${}^{3}P^{40}_{3.5}$	21.0	17.9	18.0
${}^{4}P^{40}_{3.5}$	21.1	17.1	16.6

3.5. Influence of the meq complex/g of clay ratio

Table 4 shows the values of d(001) of the montmorillonite pillared with different quantities of the iron complex solution.

A marked effect was observed when varying the meq complex/g of clay ratio, especially when this ratio was low. In this case, a solid with poor thermal stability is obtained. A maximum was found when 3.5 or 4.5 ratios were used, however, solid ${}^{3}P^{40}_{3.5}$ (ratio = 3.5) shows a better thermal stability.

From the above results, the optimum conditions for having a solid with high thermal stability were: temperature of exchange: 40°C, time of exchange: 3 h and meq complex/g of clay ratio: 3.5.

Thermal stability of the solid prepared using such conditions was studied. The intensity of the diffracted X-ray beam in the region of the 001 reflections is shown for this solid in Fig. 2.

When calcination temperature was varied between room temperature and 700°C, the X-ray signal characteristic of the d(001) was maintained. Table 5 shows the basal spacing values obtained. This extraordinary thermal stability was also observed by thermo gravimetric analysis (TGA) where no additional weight loss was obtained after 300°C calcination temperature in air.

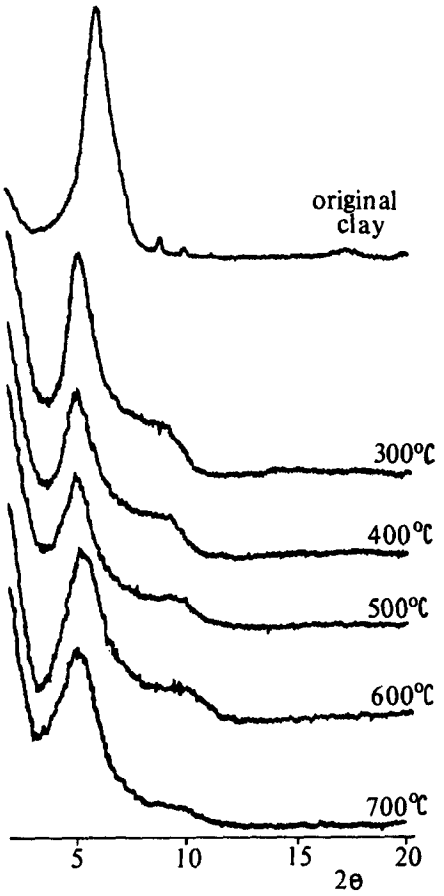

Fig. 2. Intensity of the diffracted X-ray beam in the region of the 001 reflections.

Table 4
Basal spacing in Å and its evolution with thermal treatment of the iron-pillared clays prepared. Influence of meq complex/g of clay ratio

Solid	Temperature (°C)		
	25	300	500
Original clay	14.9	–	9.6
${}^{3}P^{40}_{2.5}$	21.4	16.7	–
${}^{3}P^{40}_{3.5}$	21.0	17.9	18.0
${}^{3}P^{40}_{4.5}$	20.9	16.3	16.1

Table 5
Basal spacing for the solid ${}^{3}P^{40}_{3.5}$ calcined at temperatures between room and 700°C

Temperature (°C)	Basal spacing 001 (Å)
25	21.0
300	17.9
400	17.9
500	18.0
600	17.3
700	16.9

Fig. 3. Micrograph of $^3P^{40}_{3,5}$ solid dried at room temperature.

Fig. 4. Micrograph of $^3P^{40}_{3,5}$ solid calcined at 500°C.

3.6. Textural properties and chemical analyses of the Fe-PILC prepared

Table 6 shows the iron content and surface areas obtained for all the samples prepared.

When exchange is conducted, the surface area increases dramatically, increasing further after calcination. The iron content for most of the solids was between 28 and 31% with the only exception of $^3P^{20}_{3.5}$ and $^3P^{40}_{2.5}$ solids. It is interesting to note that this two solids are thermally unstable. This result suggests that thermal stability seems to be related to the iron content.

3.7. Characterisation of the Fe-PILC $^3P^{40}_{3.5}$

A thorough characterisation of the Fe-PILC $^3P^{40}_{3.5}$ solid was conducted in order to corroborate the incorporation of iron inside the clay.

3.8. Scanning electron microscopy

Figs. 3 and 4 show the micrographs of $^3P^{40}_{3.5}$ at room temperature and calcined at 500°C respectively. The characteristic 'finger print' structure of pillared clays can be observed in both cases which supports the presence of iron in between the layers of the clay in this solid. The basal spacing measured by this technique was the same (16 Å) for the two samples. This low value obtained is expected because the temperature at the sample increases dramatically as a consequence of the X-ray beam. The fact that there is no change in the basal spacing in these two samples provide further evidence of the thermal stability of the solid. The TEM micrograph of the solid after reduction and reaction does not show mayor changes compared with the calcined solid. This fact provide additional evidence of the thermal stability of the solid.

Table 6
Surface area of the solids prepared

Solid	Surface area (m^2/g)			
	25°C	300°C	500°C	% Fe
Original clay	34	–	–	2.8
$^3P^{50}_{3.5}$	171	187	122	28.7
$^3P^{40}_{3.5}$	220	223	205	27.7
$^3P^{30}_{3.5}$	199	254	244	28.5
$^3P^{20}_{3.5}$	198	216	143	20.0
$^1P^{40}_{3.5}$	165	239	246	30.5
$^2P^{40}_{3.5}$	197	264	262	31.0
$^4P^{40}_{3.5}$	191	247	270	28.3
$^3P^{40}_{2.5}$	172	230	260	22.4
$^3P^{40}_{4.5}$	146	233	252	26.8

Table 7
Mössbauer parameters and iron phases of the calcined at 500°C and non calcined $_3P^{40}_{3.5}$ solid

Treatment	IS (mm/s)	QS (mm/s)	Hhf (kG)	Phase	%
Non calcined	0.362	0.678		Fe^{3+}	100
	0.338	0.786	0.000	Fe^{3+}	83
Calcined 500°C	0.385	0.010	482	α-Fe_2O_3	17

3.9. Mössbauer spectroscopy

Table 7 shows the Mössbauer parameters and the iron phases present in the non calcined and calcined at 500°C $^3P^{40}_{3.5}$ catalyst.

For the non calcined solid, a symmetric doublet is observed with a IS = 0.362 mm/s and a QS = 0.678 mm/s attributed to Fe^{3+} in octahedral configuration while the calcined sample shows a composed spectrum where a symmetric doublet and a sextuplet were observed. For the doublet the IS value was 0.338 mm/s and the QS was 0.786 which indicate the permanence of Fe^{3+} (83%) after calcination. The increase of the QS value from 0.678 mm/s to 0.786 mm/s when the sample is calcined can be attributed to the change of the chemical environment of the intercalated iron. This result has also been reported by Dhar [21], Doff [23] and Martin-Luengo [24]. The sextuplet with Hhf = 482 kG, IS = 0.385 mm/s and QS = 0.010 mm/s evidence the formation of α-Fe_2O_3 (17%) in small magnetic particles. In the reduced catalyst the spectra were very similar to those obtained for the calcined sample, however, a small contribu-

Table 8
Conversion and product distribution of some of the solids prepared

Solid	% XCO	% CO_2	% CH_4	% C_2–C_4	% C_5	% C_6^+	α
Original clay	3.82	45.33	24.54	20.24	5.55	4.34	0.50
$^3P_{3.5}^{40}$	21.45	23.39	31.24	40.31	0.98	4.07	0.45
$^3P_{3.5}^{20}$	28.04	25.88	27.33	39.26	0.59	6.92	0.50
$^3P_{2.5}^{40}$	20.45	25.12	28.08	40.00	0.52	6.27	0.50

$H_2/CO = 2$; $P = 300$ psi; $T = 300°C$; $SV = 1000\ h^{-1}$.

tion of a sextuplet, characteristic of α-Fe in small particles was observed.

3.10. CO hydrogenation reaction

The catalytic behaviour of the solids prepared was assessed by the CO hydrogenation reaction. Table 8 shows the results obtained after the steady state was reached.

When the original clay is pillared, an increase of activity is observed probably related with the amount of iron present in the pillared clays, however, this relationship is non linear. The product distribution shows that for the pillared clay, the amount of CO_2 formed decreases dramatically, the selectivity towards CH_4 is higher and a high formation of the C_2–C_4 fraction is obtained.

When comparing the most stable sample with the two thermally unstable catalysts, it is observed that, even if the iron content in the latest samples is lower, their conversion is similar for the three samples. Moreover, the sample with the lowest iron loading have the highest conversion and in turn is the less thermally stable.

It is interesting to note that, after reduction and reaction, the solid $^3P_{3.5}^{40}$ was again characterized by TEM and Mössbauer spectroscopy. It could be observed that its laminar structure was almost unchanged. This fact pointed out, once again, the remarkable thermal stability of this solid.

4. Discussion

From the results obtained, two main factors are of importance in the preparation of thermally stable Fe-PILC catalysts: (i) the number of pillars formed and (ii) the degree of hydrolysis of the iron complex.

It has been reported by Figueras [28] that exchange in clays is favoured with temperature, charge and size of the cation being favoured for small cation.

When lower temperatures are used, the exchange velocity becomes slow. In this case, the number of pillars formed is small and the resulting solid should have a poor thermal stability as is indeed the case (Table 2). On the other hand, high temperature will favour the exchange velocity, however, if the temperature is too high, the hydrolysis of the iron complex is also favoured [22]. As a result, the resulting solid loses thermal stability, as observed.

The effect of the exchange time is not so marked, however, the longest time of exchange (4 h, Table 3) produced the solid with the lowest thermal stability. This fact seems to indicate that the complex was more hydrolyzed, since time also will favour hydrolysis of the complex.

The concentration of the cation in the solution (meq complex/g of clay ratio), also has great influence on the formation of a thermally stable Fe-PILC. When concentration of the cation is low, the mass transfer process is not favoured, so the exchange velocity decreases. In this case (as seen for low temperatures) the number of pillars is small, rendering the solid thermally unstable. A high concentration of the iron complex does not seem to have any influence on the final product within the studied range.

Interestingly enough, the chemical analysis

(Table 6) shows that the two samples which are thermally unstable are the samples with the lower iron content. This fact corroborates the assumption that the number of pillars formed is of primary importance for thermal stability.

The presence of iron in between the layers of the clay was evidenced. The initial increase of surface area is readily related with the creation of microporosity in the clay as reported by Fetter et al. [29]. When the samples were calcined, an additional increase of surface area was observed, probably related with the decomposition of the iron complex.

By means of transmission electron microscopy, additional evidence was found as the characteristic 'finger print' structure of pillared clays was observed. This structure was retained even after reduction and reaction.

Calcination of the free iron complex should produce its decomposition and formation of α-Fe_2O_3. The Mössbauer results obtained (Table 7) showed that, when present in the Fe-PILC, iron was mainly (83%) as Fe(III) in an octahedral configuration before and after calcination in air at 500°C. This fact not only shows clearly the incorporation of iron in between the layers of the clay, but also its great thermal stability. The presence of the sextuplet due to α-Fe_2O_3 indicates, however, that a small part of the iron goes out of the structure during calcination. The presence of α-Fe_2O_3 due to free iron complex deposited on the clay during preparation is ruled out because samples were thoroughly washed after the exchange process; furthermore, the fact that the surface area decreases in this solid after calcination at 500°C, points out that some iron is leaving the layers of the clay and is resting around the entrance of the porous. Mössbauer results on the reduced sample corroborate this statement.

The catalytic performance of the catalysts is very promising. Even if the amount of iron is increased by a factor of 10 (Table 6) for the more stable catalyst, the conversion does not increase in the same degree (Table 8). This unwanted control of activity renders the solids selective towards the C_2–C_4 fraction in the CO hydrogenation reaction. There were not marked differences in the product distribution for all the solids tested, however, for the unstable solids, conversion is higher. The poor stability of these catalysts allows that the iron (which goes out of the structure of the clay during the calcination process) becomes reduced and carbured. As reported elsewhere [30–32], iron species reduced and carbured are the main responsible for the high activity of iron in this reaction.

It is well known that product distribution is markedly dependent on conversion when working with conventional Fischer–Tropsch catalysts. The fact that it remains constant in all the solids tested regardless of it conversion could be explained by the presence in the solid of a controlled porous structure. Moreover, conventional Fe/Al_2O_3 catalysts, even promoted with K and Mn, which are known to enhance the selectivity to light olefins, are reported to give a maximum of 35% of the C_2–C_4 fraction with 20% conversion [33]. This value is lower than that obtained in the present study. These facts point out a combination of activity and shape selectivity in the Fe-pillared clays prepared in this work.

5. Conclusions

A remarkable thermally stable Fe-PILC catalyst has been prepared with surface areas between 200 and 270 $m^2\ g^{-1}$ and basal spacing of around 21 Å when dried at room temperature. Two main factors are responsible for attaining this high thermal stability, the number of pillars in between the layers of the clay and the degree of hydrolysis of the iron complex. The high thermal stability reached with this solids limited the catalytic activity. However, this unwanted control of activity renders the solids selective towards the C_2–C_4 fraction in the CO hydrogenation reaction, making the study of this kind of solids very promising.

References

[1] A. Weiss, Angew. Chem. Ind. Ed. Engl., 20 (1981) 850.
[2] M.M. Mortland and V.E. Berkheiser, Clays Clay Minerals, 24 (1976) 60.
[3] T.J. Pinnavaia, M.S. Tzou, S.D. Landau and R.H. Raythatha, J. Mol. Catal., 27 (1984) 195.
[4] M.L. Occelli, Catal. Today, 2 (1988) 339.
[5] Ming-H. Yuan, L. Zhonghui and M. Ense, Catal. Today, 2 (1988) 321.
[6] E. Kikuchi, T. Matsuda, J. Veda and Y. Morita, Appl. Catal., 16 (1985) 401.
[7] T. Matsuda, M. Matsukata, E. Kikuchi and Y. Morita, Appl. Catal., 21 (1986) 297.
[8] R. Burch and C.I. Warburton, J. Catal., 97 (1986) 511.
[9] T.J. Pinnavaia, M.S. Tzou and S.D. Landau, J. Am. Chem. Soc., 107 (1985) 2783.
[10] G.J.J. Bartley, Catal. Today, 2 (1988) 233.
[11] C.I. Warburton, Catal. Today, 2 (1988) 271.
[12] N.D. Skoularikis, R.W. Coughlin, A. Kostapapas, K. Carrado and S.L. Suib, Appl. Catal., 39 (1988) 61.
[13] H.L. Del Castillo and P. Grange, Appl. Catal., 103 (1993) 23.
[14] R. Molina, A. Schutz and G. Poncelet, J. Catal., 145 (1994) 79.
[15] M.S. Tzou, Ph.D. Thesis, Michigan State Univ., 1983.
[16] W.Y. Lee, R.H. Raythatha and B.J. Tatarchuk, J. Catal., 115 (1989) 159.
[17] V.E. Berkheiser and M. Mortland, Clays Clay Minerals, 25 (1977) 105.
[18] S.M.F. Traynor, M. Mortland and T.J. Pinnavaia, Clays Clay Minerals, 26 (1978) 318.
[19] R.H. Loeppert, M.M. Mortland and T.J. Pinnavaia, Clays Clay Minerals, 27 (1979) 201.
[20] S. Yamanaka, T. Sako and M. Hattori, Mater. Res. Bull., 19 (1984) 161.
[21] M. Dhar, M. Vittal and T.G. Narendra, Proc. 7th Int. Zeolite Conf., Tokyo, 1986, p. 154.
[22] S. Yamanaka and M. Hattori, Catal. Today, 2 (1988) 261.
[23] D.H. Doff, N.H.J. Gangas, J.E.M. Allan and J.M.D. Coey, Clay Minerals, 23 (1988) 367.
[24] M.A. Martin-Luengo, H. Martins-Carvalho, J. Ladrieve and P. Grange, Clay Minerals, 24 (1989) 495.
[25] R. Burch and C.I. Warburton, Appl. Catal., 33 (1987) 395.
[26] Y. Kiyosumi, K. Suzuki, S. Shin, K. Owaga, K. Saito and S. Yamanaka, Japan Kokai Tokyo Koho, 1984, 59-216631.
[27] E. Pretsch, T. Clerc, J. Seibl and W. Simon, Tables for Structural Elucidation of Organic Compounds by Spectroscopic Methods, Alhambra, 1980.
[28] F. Figueras, Catal. Rev. Sci. Eng. 30 (1988) 457.
[29] G. Fetter, D. Tichit, P. Massiani R. Dutartre and F. Figueras, Proc. XII Iberoamerican Symp. Catal., 2 (1990) 448.
[30] M.R. Goldwasser, F. Navas, M.J. Pérez Zurita, M.L. Cubeiro, E. Lujano, C. Franco, F. González-Jimenez, E. Jaimes and D. Moronta, Appl. Catal., 100 (1993) 85.
[31] M.R. Goldwasser, M.L. Cubeiro, M.J. Pérez Zurita and C. Franco, in L.F. Guczi Solymosi and P. Tétényi (Eds.), Proc. 10th ICC, Elsevier, Amsterdam, 1993, p. 2095.
[32] M.L. Cubeiro, M.R. Goldwasser, M.J. Pérez Zurita, C. Franco, F. González-Jimenez and E. Jaimes, Hyperfine Interactions, 93 (1994) 1831.
[33] M.L. Cubeiro, G. Valderrama, M.R. Goldwasser, F. González-Jimenez, M.C. Da Silva and M.J. Pérez Zurita, to be presented at the Fourth International Natural Gas Conversion Symposium, Kruger National Park, South Africa, November 1995.